PHYSICAL REVIEW C **80**, 065810 (2009)

The $^{17}F(p,\gamma)^{18}Ne$ resonant cross section

K. A. Chipps*
Colorado School of Mines, Golden, Colorado 80401 USA
and Rutgers University, New Brunswick, New Jersey 08901 USA

D. W. Bardayan, C. D. Nesaraja, and M. S. Smith
Oak Ridge National Laboratory, Oak Ridge, Tennessee 37831 USA

J. C. Blackmon
Louisiana State University, Baton Rouge, Louisiana 70803 USA

K. Y. Chae, B. H. Moazen, and S. T. Pittman
University of Tennessee, Knoxville, Tennessee 37996 USA

U. Greife
Colorado School of Mines, Golden, Colorado 80401 USA

R. Hatarik and W. A. Peters
Rutgers University, New Brunswick, New Jersey 08901 USA

R. L. Kozub and J. F. Shriner Jr.
Tennessee Technological University, Cookeville, Tennessee 38505 USA

C. Matei
Oak Ridge Associated Universities, Oak Ridge, Tennessee 37830 USA

S. D. Pain
Oak Ridge National Laboratory, Oak Ridge, Tennessee 37831 USA
and University of Tennessee, Knoxville, Tennessee 37996 USA
(Received 10 August 2009; published 31 December 2009)

We directly measure the $^{17}F(p,\gamma)^{18}Ne$ resonant reaction using a mixed beam of ^{17}F and ^{17}O at the Holifield Radioactive Ion Beam Facility at Oak Ridge National Laboratory (ORNL). The astrophysically important 3^+ resonance at ~600 keV above the proton threshold in ^{18}Ne is found to have a partial width $\Gamma_\gamma = 56 \pm 24(\text{stat}) \pm 30(\text{sys})$ meV, in reasonable agreement with the theoretically predicted width. A 2σ upper limit on the direct capture of $S(E) \leqslant 65$ keV b is determined at an energy of 800 keV. Experimental techniques and astrophysical implications are discussed.

DOI: 10.1103/PhysRevC.80.065810 PACS number(s): 25.40.Ny, 26.30.−k, 26.50.+x, 27.20.+n

I. INTRODUCTION

Within explosive astrophysical environments the rates of nucleosynthesis reactions control both the energy generation and isotope production, making them critical to measure. Specifically, the $^{17}F(p,\gamma)^{18}Ne$ reaction is of significant importance in such astrophysical scenarios as novae and x-ray bursts. The decay of ^{17}F, with a half-life of ~1 min, is thought to drive the late expansion of a nova envelope [1]. Another isotope of fluorine, ^{18}F, is mainly produced through β-decay of ^{18}Ne and proton capture on ^{17}O [1,2]. It is destroyed through $^{18}F(p,\alpha)^{15}O$ [3] and β-decay to ^{18}O in astrophysical scenarios where large quantities of the hot-CNO cycle nuclei ^{13}N, $^{14,15}O$, and $^{17,18}F$ exist, such as novae [4]. The two annihilation γ-rays from this ^{18}F β-decay could be directly observed by γ-ray telescopes such as GLAST or INTEGRAL because the half-life of ^{18}F (approximately 110 min) is relatively long compared to nova time scales, which allows the ^{18}F to survive until the nova envelope becomes more transparent [5]. However, the amount of ^{18}F produced in novae is uncertain in part because of the previously unmeasured $^{17}F(p,\gamma)^{18}Ne$ rate. At lower temperatures the reaction sequence $^{17}F(e^+\nu_e)^{17}O(p,\alpha)^{14}N(p,\gamma)^{15}O(e^+\nu_e)^{15}N$ contributes to the observed overabundance of ^{15}N in novae ejecta [5]. This reaction sequence is of interest as novae are thought to be important contributors to galactic ^{15}N abundances. At temperatures above about 0.2 GK, depending on the density of the novae environment, the $^{17}F(p,\gamma)^{18}Ne(e^+\nu_e)^{18}F$ reaction chain becomes important as it increases production of ^{18}F and therefore alters the ratio of ^{18}F to ^{17}F abundances. Thus the rate

*Current address: University of York, Heslington, UK YO10 5DD.

of proton capture on ^{17}F in this temperature regime is crucial to the understanding of the production of several important astronomical observables in novae.

The sequence ^{14}O$(\alpha,p)^{17}$F$(p,\gamma)^{18}$Ne$(\alpha,p)^{21}$Na initiates the α–p chain during an x-ray burst [1]; this reaction sequence increases the rate of energy generation by 2 orders of magnitude [6] and allows for rp-process synthesis of nuclei heavier than Fe [7]. Two peaks in energy production are found in simulations of the preburst phase of an x-ray burst event, one spike being caused by "the conversion of ^{16}O into ^{15}O initiated by two subsequent proton capture reactions," which "depends on the ^{17}F$(p,\gamma)^{18}$Ne rate" [8]. In each of the burst scenarios considered between 10% and 100% of the total flux was found to proceed through the ^{17}F$(p,\gamma)^{18}$Ne reaction [8]. Additionally, further simulations showed the final abundances of several nuclei produced in x-ray burst scenarios to be altered significantly based on the assumed ^{17}F$(p,\gamma)^{18}$Ne rate [2]. This indicates that the ^{17}F$(p,\gamma)^{18}$Ne reaction is crucial to preburst energy generation during x-ray bursts as well as changes in final isotopic abundances.

Our understanding of these violent astrophysical scenarios is thus partially dependent on knowledge of the ^{17}F$(p,\gamma)^{18}$Ne reaction, but the proton capture rate on ^{17}F remained unmeasured experimentally until recently [2]. It is now known that a broad, low energy 3^+ state in ^{18}Ne (an s-wave transfer from the ^{17}F ground state), in combination with direct capture, dominates the cross section at the temperatures typical of the astrophysical scenarios described earlier [2]. Such a state was predicted based on a known mirror state in ^{18}O [9]; several theoretical predictions are shown in Fig. 1. Previous studies of the relevant energy region near an excitation energy of about 4.3 MeV in ^{18}Ne included the ^{16}O$(^3$He,$n)^{18}$Ne [11–18], ^{20}Ne$(p,t)^{18}$Ne [11,13–17,19,20], ^{12}C$(^{12}$C,^{6}He$)^{18}$Ne [17], and ^{17}F$(p,p)^{17}$F [1,5] reactions. The ^{17}F(p,p) study was the first to conclusively observe this 3^+ state in ^{18}Ne, suggesting the level is largely of ^{17}F + p structure. The resonance was located at an energy of 599.8 ± 2.0 keV above the proton threshold ($E_x = 4523.7$ keV) with a total width of $\Gamma = 18 \pm 2$ keV.

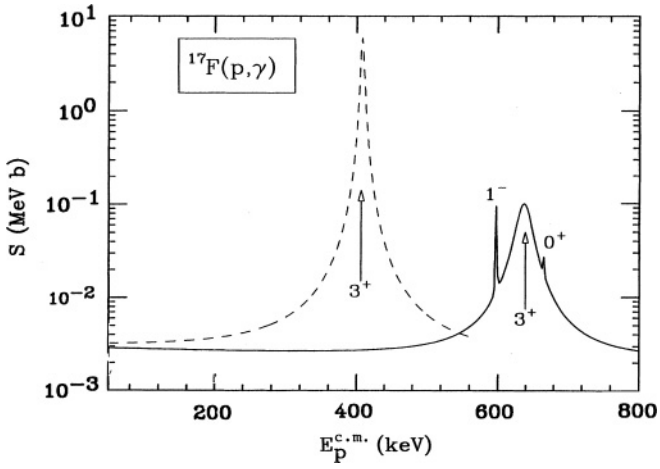

FIG. 1. Astrophysical S factor for the ^{17}F proton capture; the dashed line is the expected curve for the state predicted by Wiescher *et al.* [9] and the solid curve is calculated by García *et al.* [10] for the same predicted state. The figure is originally from Ref. [10].

A subsequent high-resolution ^{16}O$(^3$He,$n)$ experiment [18] assigned parameters that agreed well with the ^{17}F(p,p) measurement. However, both the 3^+ resonance strength and the direct capture cross section thought to dominate at nova temperatures [1,21] remained, at that point, experimentally unknown. Subsequent theoretical shell-model calculations predicted a partial γ width for the 3^+ state of 25 ± 16 meV [10] and a cluster model predicted a similar value of 33 meV [22]. The uncertainty quoted by García *et al.* [10] was based upon experimental lower limits of the mirror transition in ^{18}O, but in both cases no account of the inherent uncertainties in the theoretical prediction was made. Similarly, no uncertainties existed on predictions for the direct capture cross section.

Because of the lack of experimental information Iliadis *et al.* [23] assigned an estimated uncertainty to the ^{17}F$(p,\gamma)^{18}$Ne reaction rate in the region of nova temperatures of plus or minus a factor of 10 for their sensitivity study. Since the proton widths for the ^{18}Ne states above the ^{17}F + p threshold are much larger than the γ widths ($\Gamma_\gamma \ll \Gamma_p$), the resonance strength $\omega\gamma$ is directly proportional to the partial width Γ_γ. As the resonant reaction rate therefore depends directly on the partial width Γ_γ, it is a critical parameter to measure. The total rate is dominated in this temperature regime by the 3^+ resonance contribution and direct capture so once the properties of the levels involved in both the direct and resonant captures are known the reaction rate can be calculated. In this article we will discuss in detail a direct measurement of the strength of the astrophysically important 599.8 keV resonance, the essential results of which were reported previously [2].

II. EXPERIMENT

A. Setup

Utilizing a ^{17}F beam produced at the Holifield Radioactive Ion Beam Facility (HRIBF) at Oak Ridge National Laboratory (ORNL) in conjunction with the Daresbury Recoil Separator (DRS), the ^{17}F$(p,\gamma)^{18}$Ne proton capture reaction was measured directly. A beam comprised of both ^{17}F, typically ∼35%–70% of the total, and stable ^{17}O was produced at the HRIBF. This mixed beam was then accelerated using the 25 MV tandem accelerator into a differentially pumped, windowless H_2 gas target (WGT) [24], which was similar to a design used by the Napoli Bochum Nuclear Astrophysics (NABONA) collaboration [25]. The WGT was well characterized in a recent ^{7}Be(p,γ) experiment [24]. The pressure of the H_2 gas within the central disk of the target was set to 4 Torr and controlled to within 0.002 Torr creating an effective length of 19.5 cm. The pressure at the center of the target disk can be up to 5 Torr of H_2 while still allowing the pressures at the entrance and exit apertures to be low enough to connect to the rest of the beamline (in the 10^{-6} Torr range or below). Inert gases such as the ^{20}Ne used to examine elastic scattering (see below and Fig. 5) can be used at pressures of 10 Torr or higher. The first downstream aperture of the WGT was designed such that essentially all recoils will pass through unobstructed; for this measurement the aperture was 30% wider than necessary to allow for 100% transmission of the recoiling ^{18}Ne.

To measure the reaction cross section, the beam current was monitored using two independent methods. First, doubly

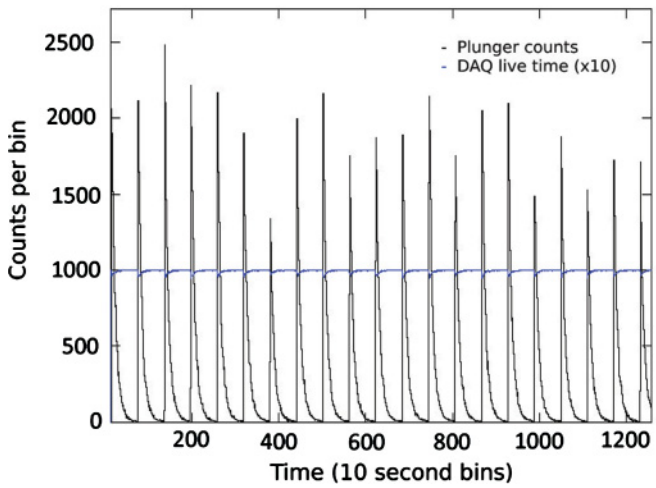

FIG. 2. (Color online) Representative spectrum from the "plunger" beam-current monitor. The (black) dark curve is the characteristic signal from the scintillator paddles in coincidence, showing a spike and decay each time the plate is retracted from the beam axis. The (blue) light curve displays the live time of the data acquisition system.

collimated Si surface barrier detectors inside the central disk of the gas target detected protons elastically scattered by the beam (both beam constituents). From the measured yield of scattered protons the ^{17}F beam rate could be deduced after correcting for beam purity, which was monitored continuously from the "leaky" beam that was transmitted through the DRS. To account for any subtle changes in the beam tune, the sum of two detectors, one at 45° above the beam axis and one at 45° below it was used for the calibration. Second, an additional, new beam sampling setup, sensitive only to the ^{17}F, was used. It was composed of two plastic scintillator paddles on either side of a pneumatically controlled actuator, or "plunger," that was installed just above the beamline. The pneumatic actuator, controlled via a timing-circuit box, repeatedly moved a metal plate (either Al or Cu) into the beam for a short period (10 s) to sample the beam current, then retracted the plate between the two scintillator paddles (located outside of the beamline vacuum) for a longer period (10 min) to count the ^{17}F decays. A representative spectrum is shown in Fig. 2; the two annihilation 511 keV photons detected in coincidence in the plastic scintillators were the characteristic signature of the decay of a radioactive ^{17}F beam particle implanted on the plate and so the number of photons detected in a given cycle determined the amount of impingent ^{17}F. The locations of these detectors in relation to the WGT is shown in Fig. 3. Both of the beam current measurements were calibrated by correlating their count rates to a measurement of the rate of F nuclei in the ionization chamber at the focal plane.

The charge-state fractions of the ^{17}F beam were measured after exiting the WGT by tuning selectively through the DRS and counting with the ionization chamber to determine the ratio of charge state 3+ to the full beam current (as measured without gas in the target). The DRS was then tuned to transmit the $q = 3+$ beam to the focal plane while the beam monitors recorded so a calibration between $^{17}F^{3+}$ (and

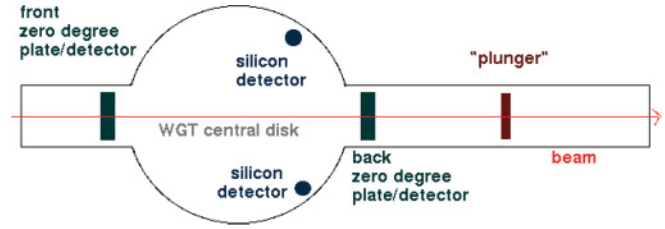

FIG. 3. (Color online) Schematic of the location of each of the beam monitoring detectors (see text).

thus total ^{17}F) at the focal plane and beam monitor count rate was found empirically. This method for calibrating beam current with monitor count can thus be performed without requiring knowledge of, for example, the total solid angle of the Si detectors in the WGT central disk, the scattering cross section of the beam constituents, or the efficiency of the plastic scintillators. The result was a calibration factor in a *number of* ^{17}F *particles per second per count in the beam monitor spectrum*, which, when summed over both the total number of counts in each monitor spectrum and the live time of the run, gave the total number of ^{17}F ions delivered during the time that spectrum was recorded. Since data were taken for several days and the beam was sampled at ten-minute intervals, any long term variations in the beam current that can significantly affect the result will be observed and accounted for by these samples. Short-term variations in the beam current were essentially random in time with respect to plunger intervals and thus will not bias the results measured over several days. The calibration factors were checked regularly; when two subsequent calibration factors differed, a systematic uncertainty of half the difference was applied to the data collected between the calibration runs. For the Si detectors inside of the WGT central disk, the uncertainty depended mainly upon the uncertainty in the ratio of beam constituents as measured in the ionization chamber (IC). The beam currents as calculated from the Si monitor detectors were consistent (but correlated) underestimates of the respective plunger calibration values; so, with the two separate methods for beam current normalization, an additional systematic uncertainty had to be introduced in our extracted resonance strength to account solely for the difference in the resonance strength values derived from each independent method. Because each method for beam current normalization was independent of the other and neither was preferred *a priori*, no weighting was applied when combining the two values.

In inverse kinematics, the resulting ^{18}Ne nuclei from the ^{17}F(p,γ)^{18}Ne reaction were very forward-focused with a maximum recoil cone of 0.443° in the laboratory frame, well within the acceptance of the WGT exit apertures and the DRS beam optics. Both the ^{18}Ne recoils and unreacted ^{17}F and ^{17}O of the beam exited the WGT into the DRS [26,27]. The DRS was tuned to transmit the ^{18}Ne recoils unobstructed to the focal plane, where they were detected unambiguously in an ionization chamber containing three anodes, a Frisch grid, and between 6 and 18 Torr of isobutane gas (depending on beam energy) [28]. By applying the usual method of plotting the

energy loss of the particles versus total energy, the recoils of interest were easily distinguished from the scattered beam.

B. Stable beam tests

Transmission studies and tests of the experimental system were performed by measuring various resonances in the $^{17}O(p,\gamma)^{18}F$ reaction, since stable ^{17}O beam was readily available at much higher beam intensities. Full (100%) transmission of beam particles can be directly checked by correlating the count rate in each of the two 0% detectors (either Faraday cups for use with the higher stable-beam intensities or Si surface barrier detectors for the lower intensity radioactive beam) mounted in the beamline on either side of the WGT (see Fig. 3), with the count rate in the focal-plane ionization chamber when these detectors were retracted off the beam axis. Cross-correlations between predicted and measured charge-state fractions for several beam energies and WGT pressures were determined. The excellent separation of particle groups was demonstrated in the appropriate energy range using the 557 keV resonance in $^{17}O + p$ [29], as shown in Fig. 4. The expected location of ^{18}Ne recoils in the ionization chamber spectrum was determined by elastically scattering ^{20}Ne gas from the WGT with an ^{17}O beam and tuning the DRS for ^{20}Ne recoils of the same energy. Figure 5 shows the spectrum from the elastic scattering measurement. It should be noted that the ionization chamber gain differs between the spectra in Figs. 4 and 5 and between these two and the later spectra (Fig. 6). The broad 1178 keV resonance in ^{18}Ne, which corresponded to a more favorable beam energy for tuning through the HRIBF tandem accelerator, was also used to test the operational parameters of the DRS, including the positioning of slits and optimizing of the magnet controls.

Furthermore, the experimental setup was checked with a measurement of the well known 1036.5 keV resonance in $^{17}O(p,\gamma)^{18}F$. A beam of 18.65 MeV ^{17}O was tuned from the tandem and into the WGT, which accounted for energy loss and centered the narrow (<1 keV) resonance inside the central disk. This state is narrow, relatively strong, and well separated from neighboring states [29] making it an ideal test for the experimental setup. The DRS was then tuned for recoil ^{18}F ions, which were detected in the focal-plane

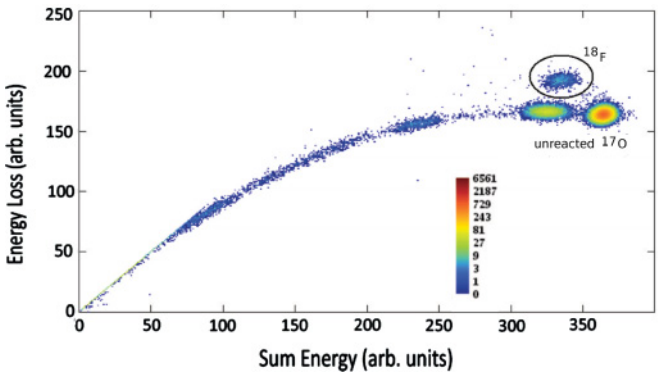

FIG. 4. (Color online) Energy loss versus total energy from the ionization chamber for the 557 keV resonance in $^{17}O(p,\gamma)^{18}F$.

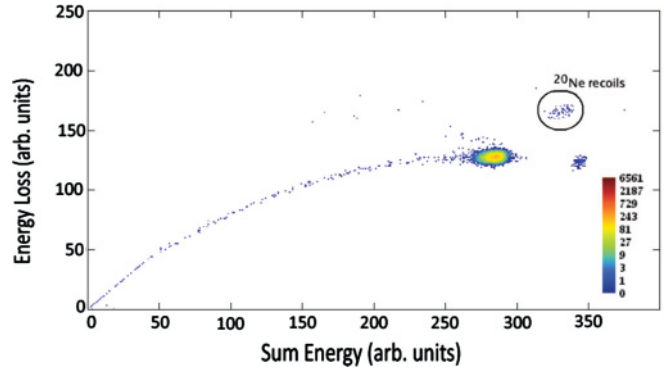

FIG. 5. (Color online) Ionization chamber spectrum for the $^{17}O + {}^{20}Ne$ scattering measurement with Ne recoils indicated; performed to verify the location of ^{18}Ne recoils during the $^{17}F(p,\gamma)^{18}Ne$ experiment.

ionization chamber. The tune of the DRS was varied slightly to search for any improvements in transmission, but none were found and the best tune was consistent with standard DRS settings. The charge-state distribution of recoil ^{18}F ions was measured by successively tuning the DRS for each charge state and measuring the relative yield. The dependence of the charge-state fractions on the gas target pressure was investigated by measuring the yield of $q = 7+$ ^{18}F ions as a function of the gas target pressure. This yield was found to be relatively constant for pressures higher than 3.5 Torr, indicating that small pressure variations in the target will not substantially affect the result (this was applied to the radioactive beam measurements as well). The beam current was determined by counting protons scattered from the H_2 target into the collimated Si detectors within the central disk. This scattering rate was calibrated by measuring simultaneously the counting rate in the detectors while a known beam current passed through the target.

The DRS was tuned for both the strongest charge state ($q = 7$; 57% of the total), and the second strongest ($q = 6$; 33% of the total) and the yield of ^{18}F recoils was measured. Combining these two charge states and accounting for uncertainties in the charge-state fraction, yield, and energy loss

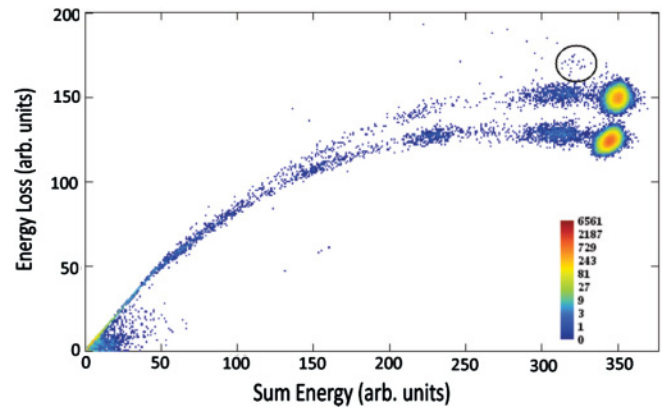

FIG. 6. (Color online) Energy loss versus total energy from the ionization chamber for the 599.8 keV resonance; ^{18}Ne recoils are indicated by the black circle.

resulted in a resonance strength of $\omega\gamma = 0.31 \pm 0.04$ eV, which is in excellent agreement with the previously adopted value of 0.36 ± 0.10 eV [29].

C. ^{17}F(p,γ)^{18}Ne

For the ^{17}F(p,γ)^{18}Ne reaction, a radioactive ^{17}F beam was tuned through the tandem at a beam energy of 14.3 MeV, which corresponded to a center-of-mass energy of 800 keV, a location far from the tails of either the 600 or 1178 keV broad resonances in ^{18}Ne. This off-resonance energy was chosen to study the background that may be present in our on-resonance runs and to set an upper limit on the direct capture cross section. Data were recorded for the two strongest charge-state fractions. The target had a thickness of 16.2 ± 1.6 keV in the center of mass at this beam energy and theoretical model predictions [10,22] agreed that the direct capture component should essentially be a constant value of ~3 keV b over the energy range inside the target. Based on the yield measured at this energy, an experimental two-σ upper limit on the astrophysical S factor off resonance was determined to be $S(E) \leqslant 65$ keV b, which is consistent with all theoretical predictions.

The yield was then measured directly at a beam energy of 10.83 MeV, corresponding to the 599.8 keV astrophysically significant 3^+ state in ^{18}Ne as shown in Fig. 6. Data were recorded with beam currents ranging between ~1–10 million ^{17}F/s, as monitored during the experiment, for a total of nearly 90 hours. At this beam energy, the target was semi-empirically determined to be 16.6 ± 1.7 keV wide (92% of the total resonance width) by matching semi-empirical stopping power predictions to measured stopping powers [24], which were scaled to correct for the beam particle and energy. Based on information gathered during the stable beam tests as well as tests with the radioactive beam the resonance was centered within the WGT central disk and the recoils centered in the IC at the focal plane of the DRS with no transmission loss. The uncertainties in both the resonance energy and the total width of the resonance were accounted for and had little effect in the final resonance strength calculation: <1% and 9%, respectively. Three different charge states of ^{18}Ne recoils were measured by tuning each individually through the DRS to experimentally determine the ^{18}Ne recoil charge-state distribution. The measured charge-state distribution was then fit to a Gaussian and extrapolated to a full distribution (i.e., integrated over all charge states), which provided the raw on-resonance yield as demonstrated in Fig. 7; the uncertainties in the fit due to the uncertainties in each measured charge state corresponded to the total yield uncertainty [30]. The net yield was calculated by first subtracting the ~20% background as estimated from the off-resonance measurement; the origin of the off-resonance counts was unclear, so the background contribution was estimated by scaling with beam current. The relatively small estimated yield from the nearby 1^- resonance ($\Gamma_\gamma = 15$ meV) [10] (see Table I) was also subtracted. The total yield due to the 3^+ resonance was thus determined, which resulted in a resonance strength of $\omega\gamma = 33 \pm 14(\text{stat}) \pm 17(\text{sys})$ meV [2]. The systematic uncertainty is dominated by uncertainty in the beam-current normalization, as discussed previously. Based on this strength, a partial width of $\Gamma_\gamma = 56 \pm 24(\text{stat}) \pm 30(\text{sys})$ meV was found, larger than, but consistent with the values predicted by theoretical calculations [10,22,31] (accounting for uncertainty). A more precise measurement would be necessary both for the resonant contribution and the direct capture to determine any discrepancies between experimental values and theoretical predictions.

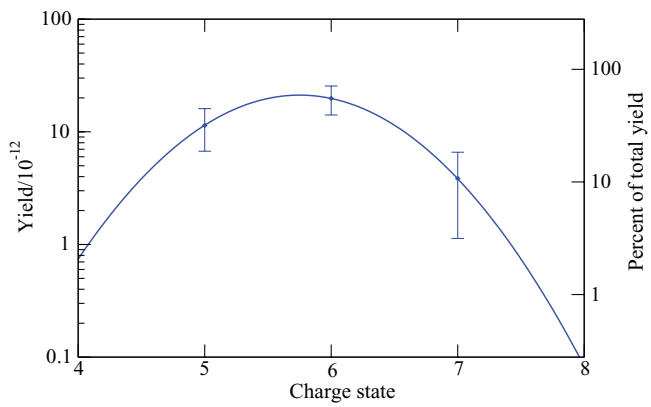

FIG. 7. (Color online) Experimentally determined charge-state distribution for the ^{18}Ne recoils from the 599.8 keV resonance. (Blue) curve is a Gaussian fit to the data.

TABLE I. Resonance parameters used for the reaction rate calculation.

E_{cm} (keV)	J^π	Γ_p (keV)	Γ_γ (meV)
597 ± 5[a]	1^-	0.1[a]	15 ± 3[a]
599.8 ± 2[b]	3^+	18 ± 2[b]	56 ± 38[c]
665 ± 5[a]	0^+	1.0[a]	1.0 ± 0.2[a]

[a]From Ref. [10].
[b]From Ref. [1].
[c]Current work (see also Ref. [2]).

III. ANALYSIS AND REACTION RATE

The ^{17}F(p,γ)^{18}Ne reaction rate calculation was improved by utilizing the newly measured experimental γ-ray width [2] with a combined (total) uncertainty, the resonance energy and total width determined by the elastic scattering measurement [1], and information on two other weak, narrow resonances near this 3^+ state [10]. The resonance parameters are listed in Table I and the reaction rate was calculated as in the previous work [1]. The direct capture contribution was calculated from the García *et al.* model prediction [10] for consistency with the previously adopted rate [1], though newer predictions for the strength of the direct capture component also agree to within uncertainty in this energy/temperature range [22,32]. The reaction rate was determined to be faster than the previously calculated rate [1] above nova temperatures by a maximum factor of ~1.8 around a temperature of 1 GK because the strength of the resonance was higher than previously predicted. We find that within the temperature range of ~0.3 to 0.4 GK, both resonant and direct captures are important [2].

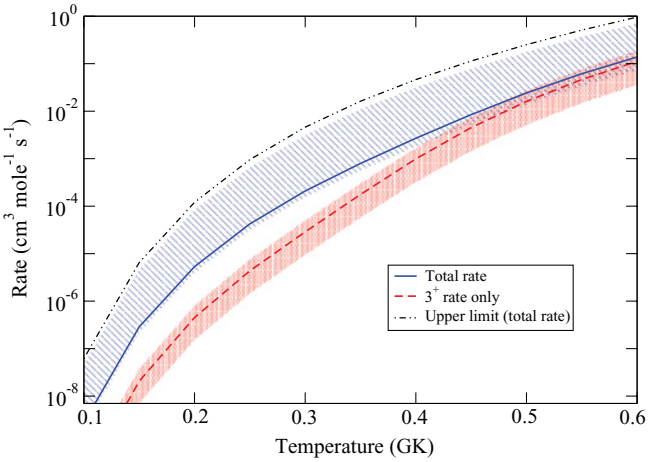

FIG. 8. (Color online) Reaction rates over the temperature range $0.1 \leqslant T_9 \leqslant 0.6$ for this work. Both the 3^+ contribution and total are shown. The (blue) diagonal hash marks display the one-σ uncertainties in the total rate from this work and the (red) dotted band indicates the one-σ uncertainties on the resonant rate alone [2]. The two-σ upper limit on the total reaction rate is also shown.

Below ~0.3 GK, direct capture is likely to still dominate the reaction rate. Significant to this measurement was the reduction of the orders of magnitude uncertainty in the previously adopted resonant rate contribution due to a lack of experimental information [23]. This uncertainty was limited to <55% for the temperature range $0.1 \leqslant T_9 \leqslant 1.0$ (where T_9 is the temperature in GK), as determined by calculating the reaction rate for the limits defined by the uncertainty in the measured partial γ width. Figure 8 shows the experimentally measured 3^+ resonant component, with the uncertainties in red. The total recommended rate [2] is shown in blue; the blue band represents the 1σ upper and lower limits in the total rate as derived solely from this work, which includes experimentally determined values for both the resonant and direct capture contributions. However, the rate indicated by the blue diagonal hash marks is not adopted as the direct capture component was not reliably extracted, and so its associated uncertainties are indicative of, but not the same as, the actual uncertainty in the total rate. While theoretical predictions do exist for the direct capture and were used previously for consistency in rate comparisons [2], it is difficult to estimate uncertainties in unmeasured quantities calculated by others and so a factor of 10 uncertainty in the direct capture rate was consequently adopted (this uncertainty is not displayed in Fig. 8). However, as several recent predictions for the direct capture are relatively consistent [10,22,32] and the uncertainty in the rate from the current resonance measurement is of the order of 55% (one σ) within the relevant temperature regime, it is unlikely that the actual direct capture rate varies by more than the suggested order of magnitude [23].

The rate, as calculated with the experimental resonant contribution and theoretical direct capture contribution was parameterized according to the Thielemann *et al.* analytic form [33] shown in Eq. (1) over the temperature range of $0.1 \leqslant T_9 \leqslant 1.0$ (where T_9 is temperature in GK):

$$N_A\langle\sigma v\rangle = \sum_{i=1}^{2}\exp\left[a_{i1} + \sum_{j=2}^{6} a_{ij}\, T_9^{2j/3-7/3} + a_{i7}\ln(T_9)\right], \quad (1)$$

using an online suite of computational tools [34] with fit residuals of less than 0.03%. The 14 coefficients calculated from the resulting parametrization are listed in Table II (this Table is also found in Ref. [2]).

TABLE II. Rate parametrization based on the Thielemann *et al.* [33] analytical form (from Ref. [2]).

Parameter	Value	Parameter	Value
a_{11}	0.275778×10^2	a_{21}	-0.784708×10^1
a_{12}	-0.495969×10^1	a_{22}	-0.323504×10^{-1}
a_{13}	-0.213249×10^2	a_{23}	-0.142191×10^2
a_{14}	-0.230774×10^0	a_{24}	0.340647×10^2
a_{15}	0.917931×10^0	a_{25}	-0.165698×10^2
a_{16}	-0.440377×10^{-1}	a_{26}	0.248116×10^1
a_{17}	-0.736014×10^1	a_{27}	-0.213376×10^1

The effect of the new resonant rate on the nova nucleosynthesis of several isotopes was further investigated by using the updated ^{17}F$(p,\gamma)^{18}$Ne rate [2] within the framework available online through the Computational Infrastructure for Nuclear Astrophysics (CINA) [34]. A "post-processing" approach was utilized (as in Ref. [21]) following a full reaction rate network with 169 isotopes from ^{1}H to ^{54}Cr through time profiles of density and temperature in one of 28 radial, one-dimensional, hydrodynamic "zones" of nova outbursts (see Ref. [34] and references therein). With the exception of ^{17}F$(p,\gamma)^{18}$Ne, the reaction rates used were the same as in Ref. [21]; the authors of that study demonstrated that the ^{17}F$(p,\gamma)^{18}$Ne reaction rate significantly affects the final abundances of many elements in a nova outburst [21].

Calculations with the parameterized rate indicate that the abundance of ^{18}F in the hottest zones of a 1.35 solar mass ONeMg white dwarf nova are increased by a factor of 1.6 over the previously adopted rate. Within the hottest zone varying the previous resonant contribution up and down by a factor of 10 as recommended by Iliadis *et al.* [23] resulted in a spread of as much as 15 to 16 times in the final abundance of ^{18}F. Using the rate derived in this work [2], along with the measured uncertainties in the resonant contribution, resulted in a range of only a factor of ~2.4, a tremendous improvement in constraining the final abundances. Simulations of the hot zone within a 1.25 solar mass white dwarf nova using the same framework resulted in a change in the final abundance range of ^{18}F from a factor of 1.6 with the previous rate and factor of ten uncertainties on the 3^+ contribution. This range was reduced to a factor of 1.15 using the current rate and resonant contribution uncertainties. Even in a small, 1.15 solar mass white dwarf, the improvement in the uncertainty in the resonant contribution provided an improvement in the uncertainty in the final ^{18}F abundances—from a factor of 1.06 to a factor of 1.01, roughly 5%—indicating the resonant rate still affects the total rate

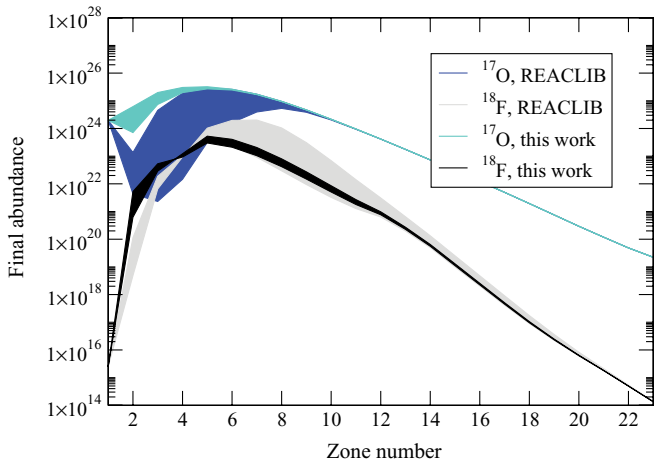

FIG. 9. (Color online) Abundance versus time for the ^{18}F (black/grey) and ^{17}O (blue/turquoise) in a 1.35 solar mass ONeMg nova. In each case, the outer lines designate the upper and lower limits from the previous rate, and the inner lines designate the upper and lower limits from this work.

down at these lower temperatures (however, it should be noted that other uncertainties may be much larger). Full 23-zone calculations of a 1.35 solar mass nova, as demonstrated in Fig. 9, showed that the final abundance of ^{18}F can vary by a factor of 7.4 with the previously recommended factor of 10 uncertainty [23] in the resonant rate alone; whereas the current rate and uncertainties (from the resonant contribution) amounted to a factor of only 1.7. Final abundances of ^{18}F in the full nova simulation were altered by a factor of ∼3 between the previous REACLIB2000 rate and current [2] rate. Similarly, for ^{17}O, the previous uncertainty is decreased from a factor of 5.6 to a factor of 1.3. The total amount of ^{17}O produced in this nova model is increased by 256% when using the current ^{17}F(p,γ)^{18}Ne rate over the previously adopted rate.

While it is important to know the effects of the ^{17}F(p,γ)^{18}Ne reaction rate on final isotopic abundances, other reactions and associated uncertainties will affect the abundances as well. To determine the extent of such effect full sensitivity studies should be performed; however, some indication can be gleaned from other recent experimental work. For example, as a byproduct of the effect of the rate measured in this work on the abundances of ^{17}O in novae, the impact of the recently measured ^{17}O(p,α)^{14}N rate is altered as well [35,36]. Because the β-decay rate is effectively constant with temperature, the region in which the ^{17}O(p,α)^{14}N rate becomes relevant is directly affected by the rate of ^{17}F proton capture. If the capture rate is faster (as was suggested by Wiescher *et al.* [9]), ^{17}O is depleted and the ^{17}O(p,α)^{14}N reaction has little effect on final abundances. If, however, the proton capture rate is weaker [1,2] the amount of ^{17}O available to react is greatly increased, subsequently increasing the importance of the ^{17}O(p,α)^{14}N reaction rate (as discussed in further detail in Ref. [36]).

Calculations of the ignition phase of an x-ray burst using the same computational framework [34], which included a reaction network of 298 isotopes coupled to exhaustive hydrodynamics, indicated that the abundances of ^{17}O and ^{17}F can be altered by an order of magnitude or more versus the

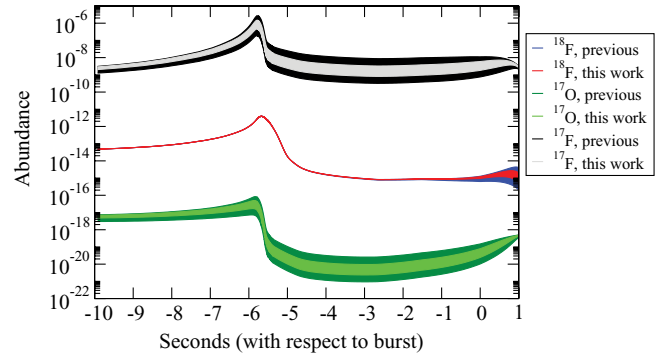

FIG. 10. (Color online) Abundance versus time for the ^{17}F (top), ^{18}F (middle), and ^{17}O (bottom) within the "ignition zone" of an x-ray burst. In each case the outer lines designate the upper and lower limits from the previous rate and the inner lines designate the upper and lower limits from this work.

previous rate [1], with reductions in uncertainty from a factor of roughly 100 to a factor of ∼5. The nature of the x-ray burst simulation is described in more detail by Roberts *et al.* [37]. Simulations with a 304-isotope network (over 3000 rates) in time for one spatial zone (the "ignition zone") of an x-ray burst were also performed. Between 2 and 4 s before the burst the ^{17}F abundances can vary by a factor of nearly 35 if the factor of 10 uncertainty in the resonant contribution was adopted and the ^{17}O abundances by a factor of 30. Using the new rate and its smaller associated uncertainties (from the resonant contribution), these factors were reduced to a spread of just under 4X for ^{17}F and a factor of 5 for ^{17}O, as shown in Fig. 10. During and after the burst (between about −0.4 and 1.2 s) the ^{18}F abundances had nearly an order of magnitude uncertainty with the previous resonant rate; with the new resonance strength and uncertainty this was reduced to a factor of ∼2. Additionally, the abundances of the two waiting-point nuclei ^{15}O and ^{18}Ne, which can have a large impact on subsequent breakout from the hot-CNO cycle into the rp-process, are altered by the reduced uncertainty in the resonant contribution: The spread in the final ^{15}O abundance is reduced from a factor of 1.23 to 1.07 and the spread in ^{18}Ne abundance from 2.1 to 1.3. Since the abundance of these two isotopes in an x-ray burst event play a crucial role in the α-p process [38], the change affected by the altered ^{17}F proton capture rate is important to quantify.

IV. CONCLUSION

The ^{17}F(p,γ)^{18}Ne reaction rate is critical to our understanding of novae and x-ray bursts. Within the relevant temperature range the 3^+ resonance at 599.8 keV in ^{18}Ne is the strongest resonant contribution. Using a mixed ^{17}F and ^{17}O beam from the HRIBF, a windowless H_2 gas target was bombarded and the ^{17}F(p,γ)^{18}Ne reaction products separated with the DRS. Based on this directly measured proton capture, a direct capture $S(E)$ factor upper limit was determined off resonance, as well as a resonance strength for the astrophysically important 599.8 keV state, which was stronger than (but consistent within uncertainties) the originally predicted strength. Experimental knowledge of this

resonance strength provides a tremendous improvement upon the uncertainties introduced by a theoretically inferred strength and was key in constraining the reaction rate of ^{17}F proton capture at and near energies found in novae and x-ray bursts. Precise determination of the ^{17}F(p,γ)^{18}Ne direct capture cross section and the ^{18}F(p,α)^{15}O reaction cross section would further reduce uncertainties in ^{18}F production in novae.

ACKNOWLEDGMENTS

ORNL is managed by UT-Battelle, LLC, for the US Department of Energy (DOE) under Contract DE-AC05-00OR22725. This work was also supported in part by the US DOE under Contract DE-FG03-93ER40789 with the Colorado School of Mines and Contracts DE-FG02-96ER40990 and DE-FG02-96ER40955 with Tennessee Technological University.

[1] D. W. Bardayan *et al.*, Phys. Rev. C **62**, 055804 (2000).
[2] K. A. Chipps *et al.*, Phys. Rev. Lett. **102**, 152502 (2009).
[3] A. St. J. Murphy *et al.*, Phys. Rev. C **79**, 058801 (2009).
[4] S. A. Glasner, E. Livne, and J. W. Truran, Astrophys. J. **475**, 754 (1997).
[5] D. W. Bardayan *et al.*, Phys. Rev. Lett. **83**, 45 (1999).
[6] M. Wiescher, H. Schatz, and A. E. Champagne, Philos. Trans. R. Soc. London A **356**, 2105 (1998).
[7] H. Schatz *et al.*, Phys. Rep. **294**, 167 (1998).
[8] M. Wiescher, J. Gorres, and H. Schatz, J. Phys. G **25**, R133 (1999).
[9] M. Wiescher, J. Gorres, and F. K. Thielemann, Astrophys. J. **326**, 384 (1988).
[10] A. García *et al.*, Phys. Rev. C **43**, 2012 (1991).
[11] J. H. Towle and G. J. Wall, Nucl. Phys. **A118**, 500 (1968).
[12] E. G. Adelberger and A. B. McDonald, Nucl. Phys. **A145**, 497 (1970).
[13] W. R. Falk, R. J. Kidney, P. Kulisic, and G. K. Tandon, Nucl. Phys. **A157**, 241 (1970).
[14] J. L'Ecuyer *et al.*, Phys. Rev. C **2**, 116 (1970).
[15] R. A. Paddock, Phys. Rev. C **5**, 485 (1972).
[16] A. V. Nero, E. G. Adelberger, and F. S. Dietrich, Phys. Rev. C **24**, 1864 (1981).
[17] K. I. Hahn *et al.*, Phys. Rev. C **54**, 1999 (1996).
[18] Y. Parpottas *et al.*, Phys. Rev. C **72**, 025802 (2005).
[19] M. S. Smith *et al.*, Nucl. Phys. **A536**, 333 (1992).
[20] S. H. Park *et al.*, Phys. Rev. C **59**, 1182 (1999).
[21] S. Parete-Koon *et al.*, Astrophys. J. **598**, 1239 (2003).
[22] M. Dufour and P. Descouvemont, Nucl. Phys. **A730**, 316 (2004).
[23] C. Iliadis *et al.*, Astrophys. J. Suppl. Ser. **142**, 105 (2002).
[24] R. Fitzgerald, Ph.D. thesis, University of North Carolina, Chapel Hill (2005).
[25] F. Strieder *et al.*, Z. Phys. A **355**, 209 (1996).
[26] A. N. James *et al.*, Nucl. Instrum. Methods A **267**, 144 (1988).
[27] R. Fitzgerald *et al.*, Nucl. Phys. **A748**, 351 (2005).
[28] A. N. James *et al.*, Nucl. Instrum. Methods **212**, 545 (1983).
[29] C. Rolfs, A. M. Charlesworth, and R. E. Azuma, Nucl. Phys. **A199**, 257 (1973).
[30] P. R. Bevington and D. K. Robinson, *Data Reduction and Error Analysis for the Physical Sciences* (McGraw-Hill, New York, 1992).
[31] R. Sherr and H. T. Fortune, Phys. Rev. C **58**, 3292 (1998).
[32] R. Chatterjee, J. Okolowicz, and M. Ploszajczak, Nucl. Phys. **A764**, 528 (2005).
[33] F. K. Thielemann, M. Arnould, and J. Truran, in *Advances in Nuclear Astrophysics*, edited by E. Vangioni-Flam *et al.*, (Editions Frontieres, Gif-sur-Yvette, 1987).
[34] M. S. Smith *et al.*, in *Proceedings of the International Symposium on Nuclear Astrophysics—Nuclei in the Cosmos IX, CERN, 2006*, edited by J. Cederkall (CERN, Geneva, Switzerland, 2006).
[35] B. H. Moazen *et al.*, Phys. Rev. C **75**, 065801 (2007).
[36] B. H. Moazen (private communication, 2009).
[37] L. F. Roberts, W. R. Hix, M. S. Smith, and J. L. Fisker, in *Proceedings of the International Symposium on Nuclear Astrophysics—Nuclei in the Cosmos IX, CERN, 2006*, edited by J. Cederkall (CERN, Geneva, Switzerland, 2006).
[38] K. Y. Chae *et al.*, Phys. Rev. C **79**, 055804 (2009).